

Intermediate-range structure of fast-ion-conducting AgI-doped molybdate and tungstate glasses

This article has been downloaded from IOPscience. Please scroll down to see the full text article.

1996 J. Phys.: Condens. Matter 8 3545

(<http://iopscience.iop.org/0953-8984/8/20/003>)

View [the table of contents for this issue](#), or go to the [journal homepage](#) for more

Download details:

IP Address: 171.66.16.208

The article was downloaded on 13/05/2010 at 16:39

Please note that [terms and conditions apply](#).

Intermediate-range structure of fast-ion-conducting AgI-doped molybdate and tungstate glasses

J Swenson[†], R L McGreevy[‡], L Börjesson[†], J D Wicks[§] and W S Howells^{||}

[†] Department of Applied Physics, Chalmers University of Technology, S-412 96 Göteborg, Sweden

[‡] Studsvik Neutron Research Laboratory, S-611 82 Nyköping, Sweden

[§] Department of Physics and Astronomy, University College, London, UK

^{||} Rutherford Appleton Laboratory, Chilton, Didcot OX11 0QX, UK

Received 8 December 1995, in final form 1 February 1996

Abstract. The structures of two fast-ion-conducting molecular glasses, $(\text{AgI})_{0.75}(\text{Ag}_2\text{MoO}_4)_{0.25}$ and $(\text{AgI})_{0.75}(\text{Ag}_2\text{WO}_4)_{0.25}$, have been investigated by neutron and x-ray diffraction. Both molybdate and tungstate glasses show a first sharp diffraction peak (FSDP) at very low Q -values (0.65 \AA^{-1} and 0.55 \AA^{-1} respectively) in the neutron data. However, only weak peaks are observed at similar Q -values in the x-ray data. The diffraction results have been used to model the structures using the reverse Monte Carlo (RMC) method. The RMC results show that all partial structure factors contribute to the FSDP except S_{AgAg} , S_{AgI} , S_{II} and S_{MoMo} (or S_{Ww}). This implies that the origin of the FSDP is somewhat different from that for the borate and phosphate glasses where S_{BB} and S_{PP} (the corresponding centres of the covalently bonded oxide groups) contribute strongly to the prepeak. The result excludes any simple explanation of the FSDP in terms of AgI clustering.

1. Introduction

To understand the ion-conducting mechanism in fast-ion-conducting glasses it is essential to know the microscopic structure in general and the environment around the mobile metal ions in particular. Several structural models have been proposed to explain the high conductivities (up to $10^{-2} \text{ S cm}^{-1}$) of metal-halide-doped fast-ion-conducting glasses. These models can be divided into two main categories depending on how the metal halide salt is distributed in the glass. The first category consists of models [1–9] based on the assumption that the metal halide salt is introduced into the host glass in clusters or micro-domains (of size $>10 \text{ \AA}$), which form connected pathways for the ions within the glass. In the second category are models where it is proposed that the dopant salt is homogeneously dispersed in the glass [10, 11]. The compositional dependence of the conductivity is then attributed either to changes in ion mobility [10] or in mobile ion concentration [11].

The diversity of assumptions in these models emphasizes the need for a better understanding of the microscopic structure. In this paper, we have used x-ray and neutron diffraction results in combination with the reverse Monte Carlo (RMC) modelling [12, 13] to investigate the structure of the two fast-ion-conducting glasses $(\text{AgI})_{0.75}(\text{Ag}_2\text{MoO}_4)_{0.25}$ and $(\text{AgI})_{0.75}(\text{Ag}_2\text{WO}_4)_{0.25}$. These glasses contain MoO_4^{2-} or WO_4^{2-} molecular ions, which do not form connected networks similar to the $-\text{BO}_3-$ and $-\text{PO}_4-$ networks in borate and phosphate glasses. In particular we have focused on the structural origin of the first sharp

diffraction peak (FSDP) observed by neutron diffraction at the anomalously low Q -values of about 0.65 \AA^{-1} and 0.55 \AA^{-1} in the molybdate [14] and tungstate glasses, respectively. A similar prepeak has been observed in other AgI-doped glasses [15, 16]. The positions of the FSDPs correspond to real-space characteristic lengths of the order of 10–12 Å. The nature of the associated intermediate-range ordering has been a matter of controversy. In the spirit of the structural models in the first category mentioned above it is proposed that it is the metal halide clusters (in this case AgI) that give rise to the FSDP [8, 9]. In [9] the authors came to the conclusion that the FSDP must be due to AgI clusters because, according to them, it is unlikely that network (e.g. AgPO_3) and molecular (e.g. Ag_2MoO_4) glasses would exhibit similar prepeaks when AgI is introduced, if it was not the AgI itself that caused the peak. However, in this paper we show that the origin of the FSDP is somewhat different for these molecular glasses to that for the network glasses studied earlier [17, 18], where the prepeak is predominantly due to local density fluctuations of the host network structure. Thus, the origin of the FSDP is not necessarily precisely the same for all types of fast-ion-conducting glasses, even if they exhibit similar prepeaks.

2. Experimental procedure

2.1. Neutron diffraction

Ion-conducting glasses with $(\text{AgI})_{0.75}(\text{Ag}_2\text{MoO}_4)_{0.25}$ and $(\text{AgI})_{0.75}(\text{Ag}_2\text{WO}_4)_{0.25}$ as their compositions were prepared by pouring their melts directly onto a copper plate cooled in liquid nitrogen. In this way small drops of the melts were quenched to glasses. These glass ‘drops’ were thereafter placed in thin-walled vanadium containers. The neutron diffraction experiments were performed using the time-of-flight Liquid and Amorphous Materials Diffractometer (LAD) at the pulsed neutron source ISIS, Rutherford Appleton Laboratory. The diffractometer has been described in detail elsewhere [19]. Time-of-flight spectra were recorded separately for each group of detectors at the angles 150° , 90° , 58° , 35° , 20° , 10° and 5° and also for monitors in the incident and transmitted beam, respectively. The data of each detector group were corrected separately for background and container scattering, absorption, multiple scattering and inelasticity effects, and normalized against the scattering of a vanadium rod following the procedure described in [20]. The corrected individual data sets obtained at each angle were then combined to obtain a large Q -range and to improve the statistics. For each data set we only used the Q -range that agreed with other data sets in the overlapping Q -region.

2.2. X-ray diffraction

X-ray diffraction experiments were performed on the same glass samples as in the neutron diffraction experiments using the high-precision powder diffractometer, Station 9.1 [21], at the Synchrotron Radiation Source (SRS), Daresbury Laboratory, UK. The glass samples were powdered and stuck on tapes. Measurements were made in transmission geometry for $2^\circ < 2\theta < 22^\circ$ and reflection geometry for $10^\circ < 2\theta < 120^\circ$. The x-ray wavelength was 0.689 \AA . After separate corrections the two spectra were scaled to overlap in the region $10^\circ < 2\theta < 20^\circ$ and combined. The inelastic Compton scattering [22] was subtracted experimentally using the Warren–Mavel method [23] (Zr K edge), as developed for use on Station 9.1 [24]. The data were also corrected for scattering from the tape, absorption and polarization, divided by the total atomic form factor and normalized to unity at large scattering angles. Multiple scattering was assumed to be negligible.

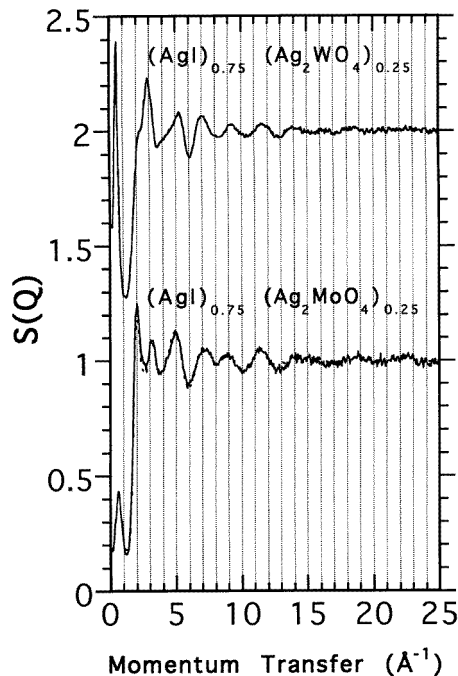


Figure 1. Experimental neutron structure factors (full lines) and computed neutron weighted total structure factors (dashed lines) for the RMC configurations of $(\text{AgI})_{0.75}(\text{Ag}_2\text{MoO}_4)_{0.25}$ and $(\text{AgI})_{0.75}(\text{Ag}_2\text{WO}_4)_{0.25}$ glasses. The curve for the tungstate glass has been shifted vertically by 1.0 for clarity.

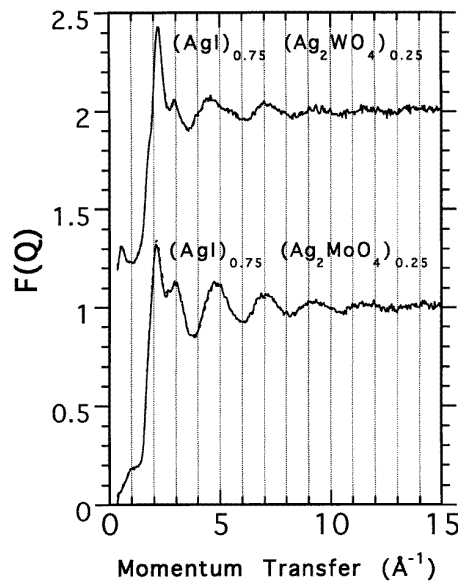


Figure 2. Experimental x-ray structure factors (full lines) and computed x-ray weighted total structure factors (dashed lines) for the RMC configurations of $(\text{AgI})_{0.75}(\text{Ag}_2\text{MoO}_4)_{0.25}$ and $(\text{AgI})_{0.75}(\text{Ag}_2\text{WO}_4)_{0.25}$ glasses. The curve for the tungstate glass has been shifted vertically by 1.0 for clarity.

3. Experimental results

3.1. Neutron diffraction

The neutron structure factors, $S(Q)$, of $(\text{AgI})_{0.75}(\text{Ag}_2\text{MoO}_4)_{0.25}$ and $(\text{AgI})_{0.75}(\text{Ag}_2\text{WO}_4)_{0.25}$ are shown in figure 1. The molybdate glass has a FSDP at a low Q -value of 0.65 \AA^{-1} and a sharp main peak at about 2.0 \AA^{-1} . Relatively sharp peaks are also observed at about 3.2 \AA^{-1} and 5.0 \AA^{-1} , due to many different (but rather well defined) interatomic distances. The tungstate displays an intense FSDP at an even lower Q -value (0.55 \AA^{-1}). The main peak is situated at about 2.9 \AA^{-1} and that is the only peak (with the exception of the FSDP) below 5 \AA^{-1} . The relatively large differences in the structure factors of the molybdate and tungstate glasses indicate that some of the interatomic distances (probably those involving Mo/W) are slightly different. The longer correlation length (i.e. the FSDP at lower Q) in the tungstate glass may be due to the slightly lower number density (about 7%), which naturally will cause an increased distance between structural groups.

3.2. X-ray diffraction

Figure 2 shows the x-ray structure factors, $F(Q)$, of $(\text{AgI})_{0.75}(\text{Ag}_2\text{MoO}_4)_{0.25}$ and $(\text{AgI})_{0.75}(\text{Ag}_2\text{WO}_4)_{0.25}$. The FSDP at 0.65 \AA^{-1} in the neutron structure factor of the molybdate has changed to a weak shoulder situated at the Q -value 0.95 \AA^{-1} . The main

peak at 2.0 \AA^{-1} in the neutron structure factor has shifted to 2.1 \AA^{-1} in the x-ray structure factor and the two other peaks at 3.2 \AA^{-1} and 5.0 \AA^{-1} are now situated at the Q -values 2.9 \AA^{-1} and 4.8 \AA^{-1} . The x-ray structure factor of the tungstate displays a FSDP at the same Q -value (0.55 \AA^{-1}) as in the neutron structure factor. The intensity of the peak is, however, strongly reduced in the x-ray structure factor. The main peak at 2.9 \AA^{-1} in the neutron structure factor is only a very weak peak here and, instead, a ‘new’ sharp and strong main peak is seen at the Q -value 2.2 \AA^{-1} in the x-ray structure factor. This Q -value corresponds to a real-space distance ($d = 2\pi/Q_{\text{peak}}$) of 2.85 \AA , which is the expected value for the nearest-neighbour Ag–I separation [25].

Table 1. Weighting factors in neutron and x-ray diffraction experiments of $(\text{AgI})_{0.75}(\text{Ag}_2\text{MoO}_4)_{0.25}$ and $(\text{AgI})_{0.75}(\text{Ag}_2\text{WO}_4)_{0.25}$ glasses. The ratios between the x-ray and neutron weighting factors are also given.

Weighting factors							
$(\text{AgI})_{0.75}(\text{Ag}_2\text{MoO}_4)_{0.25}$				$(\text{AgI})_{0.75}(\text{Ag}_2\text{WO}_4)_{0.25}$			
Atom pair	Neutron	X-ray	Ratio x-ray/neutron	Atom pair	Neutron	X-ray	Ratio x-ray/neutron
Mo–Mo	0.0084	0.0081	0.959	W–W	0.0042	0.0219	5.23
Mo–O	0.0561	0.0123	0.219	W–O	0.0408	0.0189	0.464
Mo–Ag	0.0721	0.0901	1.25	W–Ag	0.0525	0.1391	2.65
Mo–I	0.0383	0.0610	1.59	W–I	0.0277	0.0941	3.39
O–O	0.0937	0.0047	0.0499	O–O	0.0994	0.0041	0.0412
O–Ag	0.2409	0.0687	0.285	O–Ag	0.2553	0.0602	0.236
O–I	0.1279	0.0465	0.363	O–I	0.1356	0.0407	0.300
Ag–Ag	0.1549	0.2521	1.63	Ag–Ag	0.1642	0.2208	1.34
Ag–I	0.1639	0.3412	2.08	Ag–I	0.1737	0.2989	1.72
I–I	0.0436	0.1154	2.65	I–I	0.0462	0.1011	2.19

By comparing figures 1 and 2 we can see that the intensities of the two x-ray weighted FSDPs are much lower than the neutron weighted FSDPs. The reason for this is that the weighting factors in the neutron and x-ray diffraction experiments are rather different (see table 1). The correlations between Ag and I dominate strongly in the x-ray diffraction experiment, while correlations involving O are much more pronounced in the neutron diffraction experiment. Thus, the correlations involving O must contribute strongly to the FSDP.

4. Reverse Monte Carlo simulations

From the combination of neutron and x-ray diffraction experiments we have established that O must be involved in the correlations that give rise to the FSDPs. However, to obtain more insight it is necessary to perform some kind of modelling of the glass structure. This can be done by using the reverse Monte Carlo (RMC) technique [12, 13], which makes direct use of the available experimental data. RMC has recently been successfully applied to other AgI-doped ion-conducting glasses [17, 18].

4.1. The simulation procedure

The reverse Monte Carlo (RMC) simulation method [12, 13] uses a standard Metropolis Monte Carlo (MMC) algorithm [26] (including the Markov chain, periodic boundary conditions, etc) but with the ‘sum-of-squares’ difference between the measured structure

factors and those calculated from the RMC configuration as a 'driving parameter' in place of the energy. Thus, the RMC method overcomes the problem of finding accurate interatomic potentials. Data from different sources (neutron and x-ray diffraction, EXAFS) may be combined. In this way, the RMC method produces three-dimensional models of the structure of disordered materials that agree quantitatively with the available experimental data (providing that the data do not contain significant systematic errors).

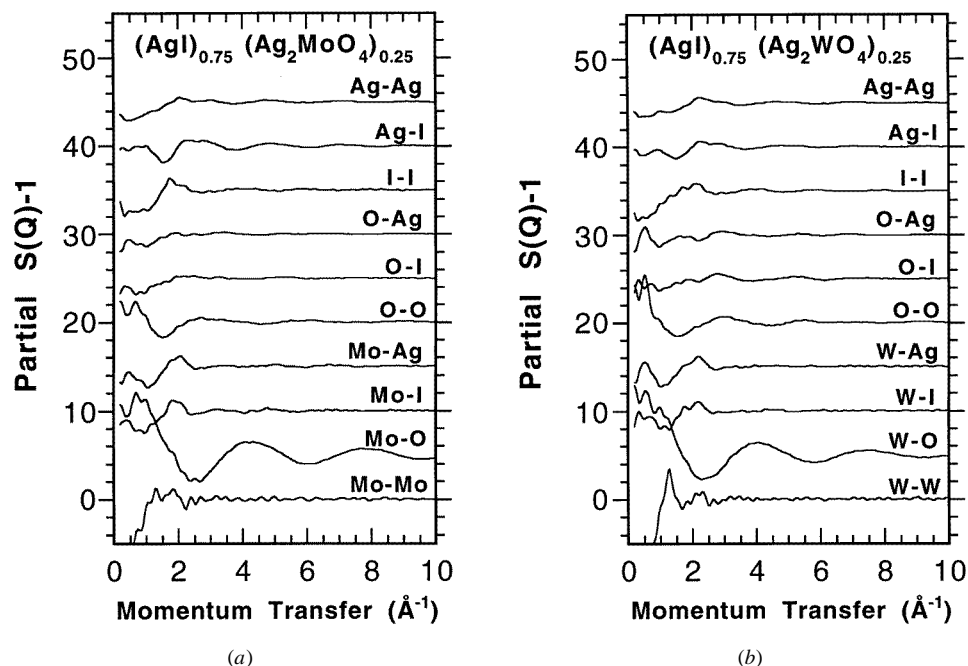


Figure 3. Partial structure factors calculated from the RMC configurations of (a) $(\text{AgI})_{0.75}(\text{Ag}_2\text{MoO}_4)_{0.25}$ and (b) $(\text{AgI})_{0.75}(\text{Ag}_2\text{WO}_4)_{0.25}$ glasses. The curves have been shifted vertically, in successive steps of 5, for clarity.

In the present case each 'computer configuration' contained 5200 atoms with atomic concentrations according to the chemical composition. Periodic boundary conditions were used and the box lengths were given values corresponding to the experimentally measured densities (5.92 g cm^{-3} for the molybdate and 5.97 g cm^{-3} for the tungstate). To be able to simulate the intermediate-range structural order the configuration has to be large enough that the corresponding box size does not influence the ordering in question, i.e. a large number of atoms must be used.

Before the actual RMC simulations were started we ran hard-sphere Monte Carlo (HSMC) simulations with certain constraints applied to ensure physically realistic configurations, in the sense that there is no overlap of atoms and that MoO_4 (WO_4) molecules are formed. The constraints were of two kinds; closest atom-atom approach and connectivity. The closest distance that two atoms were allowed to approach to was determined from experimental results, such as the radial distribution function. The only connectivity constraint was that all the Mo/W atoms should be coordinated to four oxygens. The Mo-O and W-O distances were allowed to vary between 1.65 and 2.0 Å and between 1.7 and 2.2 Å, respectively. In this way MoO_4^{2-} and WO_4^{2-} molecular ions are produced in the models.

4.2. RMC results

The structure factors of $(\text{AgI})_{0.75}(\text{Ag}_2\text{MoO}_4)_{0.25}$ and $(\text{AgI})_{0.75}(\text{Ag}_2\text{WO}_4)_{0.25}$ glasses obtained by RMC modelling are compared with those obtained experimentally in figures 1 and 2. All of the neutron and x-ray structure factors are very well reproduced. Thus, the resulting RMC-produced structural models are consistent both with the measured neutron and x-ray data and the applied constraints (in this case minimum atomic volume, sample density and fourfold Mo–O/W–O coordination). One should keep in mind that the configurations are models of the structure and that they are not unique determinations of the structure (like all other models of glass structures). However, recalling the large differences in the neutron and x-ray weighting factors (see table 1) the configurations should contain the essential structural features of the glasses investigated and in particular the information relating to the origin of the FSDPs and the type of intermediate-range order producing it.

In figures 3(a) and 3(b) we plot the partial structure factors of the configurations obtained for the $(\text{AgI})_{0.75}(\text{Ag}_2\text{MoO}_4)_{0.25}$ and $(\text{AgI})_{0.75}(\text{Ag}_2\text{WO}_4)_{0.25}$ glasses, respectively. It should be understood that since these partial structure factors are determined from self-consistent structural models any ‘errors’ are highly correlated. Consequently the partial structure factors will not be discussed in great detail; we will only discuss the trends.

The figures 3(a) and 3(b) confirm the experimental result that correlations involving O contribute to the FSDP. In fact, the RMC results show that all partial structure factors contribute to the FSDP except S_{AgAg} , S_{AgI} , S_{II} and S_{MoMo} (or S_{WW})[†]. This is somewhat different from the case for the borate and phosphate glasses where S_{BB} and S_{PP} (the corresponding centres of the covalently bonded oxide groups) contribute strongly to the FSDP [17, 18]. The high intensity in the low Q -range for S_{MoO} (or S_{WO}) and S_{OO} is mainly due to the molecular form factor, which originates from the well defined Mo–O (or W–O) and O–O distances within the MoO_4^{2-} (or WO_4^{2-}) molecules. Thus, the origin of the FSDP is somewhat different in these molecular glasses to that for the above-mentioned network glasses. However, one important similarity of these four AgI-doped glasses is evident: the partial structure factors related to Ag and I show no significant contribution to the total structure factor in the range around the FSDP; this is a necessary result given the combination of the x-ray and neutron diffraction data. This implies that structural models based on clusters of AgI [3–9] are inconsistent with the experimental results for both molecular (tungstate, molybdate) and network (borate, phosphate) glasses.

The RMC results for the molybdate and tungstate glasses can be understood in the following manner. The Mo/W distributions are effectively random, as distinct from uniform, so there are significant inhomogeneities. In regions with a higher Mo/W density, and correspondingly higher O density, there will be more ‘cross-linking’ between molecular ions via bonding to Ag^+ , e.g. by $-\text{O}-\text{Ag}-\text{O}-$ ‘bridges’. These are important since they constitute the glass network. The molecular ions in these regions will necessarily have a significant degree of orientational order. In regions with a lower Mo/W density the molecular ions will rather be separated (in a simple sense) by $-\text{O}-\text{Ag}-\text{I}-\text{Ag}-\text{O}-$ ‘bridges’ and there will be less orientational order. From the composition we would then expect an FSDP not in the partial structure factors for S_{MoMo} or S_{WW} but rather in those involving $(\text{Mo} + \text{O})-(\text{Ag} + \text{I})$ correlations, e.g. S_{MoAg} , S_{MoI} , S_{AgO} and S_{OI} , and located at a Q -value approximately half

[†] The Mo–Mo (or W–W) partial structure factor does not contribute strongly to either experimental data set (see table 1), but the fact that Mo (W) is constrained to be in a MoO_4 (WO_4) unit means that the Mo (W) position is linked to that of O which does contribute strongly. The Mo–Mo (W–W) contribution is then constrained to be effectively the same as that of the centres of the O_4 tetrahedra; the final result would not be very different even if Mo (W) had no scattering.

that of the main peak in S_{MoMo} (in crystallographic terms the local compositional fluctuations lead to a doubling of the unit cell). This is precisely what is observed. The lower Q -value for the FSDP in the tungstate glass corresponds to the slightly lower number density (about 7%), which causes the average W–W distance to be larger than the Mo–Mo distance. Note that this explanation provides a picture of the origins of the FSDP, but this is superimposed on a background of significant short-range order, and hence it is difficult to ‘see’ simply by looking at a structural model. Intermediate-range order is usually more obvious in Q -space than in r -space.

These structural findings also help to explain the relatively narrow glass composition range for these materials. To make a glass the molecular ions need to be ‘cross-linked’ in a way that allows enough disorder. For undoped Ag_2MoO_4 , for example, there is not enough flexibility and so only crystalline materials are obtained. When enough AgI has been introduced the average separation of the molecular ions increases and the number of –O–Ag–O– bridges decreases, giving more flexibility, and glasses can be formed. If too much AgI is added there are too few such bridges to constitute a network and the AgI will crystallize.

5. Summary

$(\text{AgI})_{0.75}(\text{Ag}_2\text{MoO}_4)_{0.25}$ and $(\text{AgI})_{0.75}(\text{Ag}_2\text{WO}_4)_{0.25}$, which are fast-ion-conducting molecular glasses, show diffraction peaks (FSDP) at very low Q -values (0.65 \AA^{-1} and 0.55 \AA^{-1} respectively), which are much stronger in the neutron data than in the x-ray data. The RMC results show that all partial structure factors contribute to the FSDP except S_{AgAg} , S_{AgI} , S_{II} and S_{MoMo} (or S_{WW}). This result excludes any explanation of the FSDP in terms of AgI clusters, since such clusters would have given rise to FSDPs in the partial structure factors S_{AgAg} , S_{AgI} and S_{II} .

The reason for these results is that the Mo/W atoms are effectively random, which means that their distributions are significantly inhomogeneous. Regions with a high Mo/W density, and correspondingly high O density, will have a higher degree of orientational order than regions with a low Mo/W density. This produces a FSDP, at a Q -value corresponding to twice the average Mo–Mo or W–W distance, in the partial structure factors involving (Mo + O)–(Ag + I) correlations, e.g. S_{MoAg} , S_{MoI} , S_{AgO} and S_{OI} . Thus the origin of the FSDP is somewhat different in these molecular glasses to that for in the AgI-doped network glasses, where the prepeak is predominantly due to local density fluctuations of the host network structure.

Acknowledgment

This work was financially supported by the Swedish Natural Science Research Council.

References

- [1] Carini G, Cutroni M, Fontana A, Mariotto G and Rocca F 1984 *Phys. Rev. B* **29** 3567
- [2] Ingram M D 1989 *Phil. Mag.* B **60** 729
- [3] Tachez M, Mercier R, Malugani J P and Dianoux A J 1986 *Solid State Ion.* **18–19** 372
- [4] Tachez M, Mercier R, Malugani J P and Dianoux A J 1986 *Solid State Ion.* **20** 93
- [5] Malugani J P, Tachez M, Mercier R, Dianoux A J and Chieux P 1987 *Solid State Ion.* **23** 189
- [6] Fontana A, Rocca F and Fontana M P 1987 *Phys. Rev. Lett.* **58** 503
- [7] Fontana A, Rocca F and Fontana M P 1987 *Phil. Mag.* B **56** 251

- [8] Rousselot C, Tachez M, Malugani J P, Mercier R and Chieux P 1991 *Solid State Ion.* **44** 151
- [9] Rousselot C, Malugani J P, Mercier R, Tachez M, Chieux P, Pappin A J and Ingram M D 1995 *Solid State Ion.* **78** 211
- [10] Glass A M and Nassau K 1980 *J. Appl. Phys.* **51** 3756,
- [11] Ravaine D 1985 *J. Non-Cryst. Solids* **73** 287
- [12] McGreevy R L and Pusztai L 1988 *Mol. Simul.* **1** 359
- [13] Keen D A and McGreevy R L 1990 *Nature* **344** 423
- [14] Börjesson L and Howells W S 1990 *Solid State Ion.* **40/41** 702
- [15] Börjesson L, Torell L M, Dahlborg U and Howells W S 1989 *Phys. Rev. B* **39** 3404
- [16] Tachez M, Mercier R and Malugani J P 1987 *Solid State Ion.* **25** 263
- [17] Wicks J, Börjesson L, McGreevy R L, Howells W S and Bushnell-Wye G 1995 *Phys. Rev. Lett.* **74** 726
- [18] Swenson J, Börjesson L and Howells W S 1995 *Ionics* **1** 101
- [19] Howells W S 1980, 1986 *Rutherford Appleton Laboratory Reports* RAL-80-017, RAL-86-042 (Didcot, UK)
- [20] Howe M, Howells W S and McGreevy R L 1989 *J. Phys.: Condens. Matter* **1** 3433
- [21] Bushnell-Wye G and Cernik R J 1992 *Rev. Sci. Instrum.* **63** 1001
- [22] Compton A H 1923 *Phys. Rev.* **21** 483
- [23] Warren B E and Marvel G 1965 *Rev. Sci. Instrum.* **36** 196
- [24] Bushnell-Wye G, Finney J L, Turner J, Huxley D W and Dore J C 1992 *Rev. Sci. Instrum.* **63** 1153
- [25] Nield V M, Keen D A, Hayes W and McGreevy R L 1993 *Solid State Ion.* **66** 247
- [26] Metropolis N, Rosenbluth A W, Rosenbluth M N, Teller A H and Teller E J 1953 *Phys. Chem.* **21** 1087